Re: humu-2021-0391R2

Detection of revertant mosaicism in epidermolysis bullosa through Cas9-targeted long-read sequencing

Ken Natsuga[1*†], Yoshikazu Furuta[2*†], Shota Takashima[1], Takuma Nohara[1], Hideyuki Kosumi[1], Yosuke Mai[1], Hideaki Higashi[2], Hideyuki Ujiie[1]

[1]Department of Dermatology, Faculty of Medicine and Graduate School of Medicine, Hokkaido University, Sapporo, Japan

[2]Division of Infection and Immunity, International Institute for Zoonosis Control, Hokkaido University, Sapporo, Japan

†Co-first author

***Correspondence**:

Ken Natsuga, M.D., Ph.D.

Department of Dermatology, Faculty of Medicine and Graduate School of Medicine, Hokkaido University, N15 W7, Sapporo 0608638, Japan

Tel: +81-117067387

E-mail: natsuga@med.hokudai.ac.jp

Yoshikazu Furuta, Ph.D.

Division of Infection and Immunity, International Institute for Zoonosis Control,

Hokkaido University, N20 W10, Sapporo 0010020, Japan

Tel: +81-117069547

E-mail: yfuruta@czc.hokudai.ac.jp

ABSTRACT

Revertant mosaicism (RM) is a phenomenon in which inherited mutations are spontaneously corrected in somatic cells. RM occurs in some congenital skin diseases, but genetic validation of RM in clinically revertant skin has been challenging, especially when homologous recombination (HR) is responsible for RM. Here, we introduce nanopore Cas9-targeted sequencing (nCATS) for identifying HR in clinically revertant skin. We took advantage of compound heterozygous *COL7A1* mutations in a patient with recessive dystrophic epidermolysis bullosa who showed revertant skin spots. Cas9-mediated enrichment of genomic DNA (gDNA) covering the two mutation sites (>8 kb) in *COL7A1* and subsequent MinION sequencing successfully detected intragenic crossover in the epidermis of the clinically revertant skin. This method enables the discernment of haplotypes of up to a few tens of kb of gDNA. Moreover, it is devoid of PCR amplification, which can technically induce recombination. We therefore propose that nCATS is a powerful tool for understanding complicated gene modifications, including RM.

KEYWORDS

Revertant mosaicism, epidermolysis bullosa, long-read sequencing, intragenic crossover

INTRODUCTION

Germline, or inherited, mutations are shared in most somatic cells, but revertant mosaicism (RM) is an exemption. In that case, a somatic cell undergoes spontaneous gene correction through various mechanisms such as homologous recombination (HR), second-site mutation, and back mutation. RM has been identified in multiple organs, including skin, where the clonal expansion of a revertant cell can become seen (Nomura, 2020).

Epidermolysis bullosa (EB) is a group of genetic disorders characterized by skin fragility. It is caused by mutations in the genes that encode basement membrane zone (BMZ) proteins or proteins that maintain the integrity of BMZ and adjacent keratinocytes. EB is divided into four major classical subtypes depending on the level of skin cleavage: EB simplex, junctional EB (JEB), dystrophic EB (DEB), and Kindler EB (Has et al., 2020). Some EB patients develop clinically intact skin spots that result from RM, and these spots show no skin fragility. This phenomenon has been observed in all four major EB subtypes (Almaani et al., 2010; Darling, Yee, Bauer, Hintner, & Yancey, 1999; Jonkman & Pasmooij, 2009; Jonkman et al., 1997; Kiritsi et al., 2014; Kiritsi et al., 2012; Kowalewski et al., 2016; Lai-Cheong, Moss, Parsons, Almaani, &

McGrath, 2012; Matsumura et al., 2019; Pasmooij et al., 2010; Pasmooij, Nijenhuis, Brander, & Jonkman, 2012; Pasmooij, Pas, Bolling, & Jonkman, 2007; Pasmooij, Pas, Deviaene, Nijenhuis, & Jonkman, 2005; Schuilenga-Hut et al., 2002; Smith, Morley, & McLean, 2004; Tolar et al., 2014; Twaroski et al., 2019; van den Akker et al., 2012).

At present, there is no optimal method to verify RM in clinically revertant skin spots. It has been technically challenging to detect HR, which can cause RM when the patients' mutations are compound heterozygous in autosomal recessive diseases. The problem stems from the inability to identify the alleles in which the two mutations are located at the level of genomic DNA (gDNA) since conventional sequencing technology has not allowed long reads that cover two mutation sites. An analysis at the level of complementary DNA (cDNA) has been proposed to solve this problem. It would use the sequencing of a library prepared by reverse transcription of RNA and subsequent PCR to detect HR (Matsumura et al., 2019). However, this method cannot exclude technically induced recombination by reverse transcription (Negroni, Ricchetti, Nouvel, & Buc, 1995) or polymerase in PCR reactions (Meyerhans, Vartanian, & Wain-Hobson, 1990). More importantly, when at least one of the compound

heterozygous mutations is a mutation caused by premature termination codon (PTC), nonsense-mediated mRNA decay (NMD) masks the allele housing that mutation. Therefore, a method that can analyze the sample at the level of gDNA is required for accurate verification of RM.

Single-molecule third-generation sequencing systems such as the nanopore sequencers of Oxford Nanopore Technologies and the PacBio sequencers serve as potential, significant pivots in this field because they generate long to ultra-long reads. Recently developed nanopore Cas9-targeted sequencing (nCATS) enables enrichment and sequencing of specific regions on gDNA by combining Cas9 cleavage, adapter ligation, and MinION sequencing. This allows the evaluation of haplotype-resolved single nucleotide variants at the gDNA level without PCR amplification or reverse transcription of mRNA (Gilpatrick et al., 2020). This strategy or similar ones have been utilized for detecting structural variants, copy number variants, and other somatic mutations in tumors (Gilpatrick et al., 2020; Stangl et al., 2020; Watson et al., 2020; Wongsurawat et al., 2020).

Here, we explore the feasibility of nCATS in genetically validating RM for clinically revertant skin in recessive DEB (RDEB). Although the purpose of

nCATS application to RM does not differ from its application to tumor biology, the analysis of RM is simpler than that of tumors because the latter involves diverse somatic variants. We show that HR is detected by applying this technique to gDNA without PCR amplification to confirm RM in the revertant epidermis.

MATERIAL & METHODS

RM skin

The details of the RDEB patient were described elsewhere (Natsuga et al., 2010). A 4- or 5-mm punch biopsy performed on her clinically revertant skin spots revealed no skin fragility from manual rubbing. Adjacent non-revertant skin samples with skin fragility were obtained at the same time. Two sets of the samples were processed for further analysis: one (4-mm skin) for long-range PCR and the other (5-mm skin) for nCATS. Skin samples were stored at -80 ˚C until use.

Immunofluorescence

Skin specimens were frozen on dry ice in an optimal cutting temperature (OCT) compound. The sections were fixed with cold acetone and incubated with serially diluted primary antibody LH7.2 (Sigma-Aldrich, St. Louis, MO, USA) overnight at 4 ˚C. After being washed in phosphate-buffered saline, the sections were incubated with Alexa 488-conjugated anti-mouse IgG1 (Thermo Fisher Scientific, Waltham, MA, USA) for 1 hr at room temperature. The nuclei were stained with 4’,6-diamidino-2-phenylindole (DAPI). The stained

immunofluorescent samples were observed using a confocal laser scanning microscope FV-1000 (Olympus, Tokyo, Japan).

gDNA extraction

Skin samples were incubated with 5 mM EDTA at 4 ˚C overnight, and then the epidermis and dermis were separated by scalpel. gDNA was extracted from epidermis, dermis, and peripheral blood using the Puregene Blood Core Kit (Qiagen, Valencia, CA, USA). The epidermis and dermis were frozen with liquid nitrogen and mashed with a pestle. To increase the DNA yield from the epidermis or dermis, glycogen solution (Qiagen) was added to the reaction according to the manufacturer's protocol.

PCR and plasmid construction

COL7A1 gDNA fragments (8378 bp) covering nucleotides 5932 to 8029 at the cDNA level (NM_000094.4) were amplified from epidermis, dermis, and peripheral blood gDNA using KOD one (Takara, Tokyo, Japan). The following primers were used: 5´-TCAAGGTGGGTTGTTTAGGG-3' (F) and 5´-CTACACCCCCATGACCCGAC-3' (R).

To prepare the DNA fragments for the validation experiment (**Figure 2**), the PCR products from normal human and RDEB peripheral blood gDNA were subcloned into the pCRII-Blunt-TOPO vector (Thermo Fisher Scientific), and clones with *COL7A1* sequence of WT, c.5932C>T, or c.8029G>A were isolated. The plasmids were extracted using the Plasmid Midi Kit (Qiagen, Hilden, Germany) and digested by HindIII and NotI (New England Biolabs, Ipswich, MA, USA). The fragments with cloned *COL7A1* sequence were purified using QIAquick Gel Extraction Kit (Qiagen), and then MinION sequencing was applied.

MinION sequencing of DNA fragments

Sequencing libraries were prepared following the protocol for “Native barcoding genomic DNA (with EXP-NBD104, EXP-NBD114, and SQK-LSK109)” (Version NBE_9065_v109_revK_14Aug2019). Briefly, DNA fragments were first treated with NEBNext FFPE Repair Mix and NEBNext End repair/dA-tailing Module (New England Biolabs) and were purified using AMPure XP beads (Beckman Coulter, Brea, CA, USA). The samples were ligated with the Native Barcode of Native Barcoding Expansion Kits EXP-NBD104 and EXP-NBD114 (Oxford

Nanopore Technologies, Oxford Science Park, United Kingdom), using Blunt/TA Ligase Master Mix (New England Biolabs). They were purified again using AMPure XP beads. After pooling equal amounts of the barcoded samples, Adapter Mix II of Ligation Sequencing Kit SQK-LSK109 (Oxford Nanopore Technologies) was ligated to the sample using T4 DNA Ligase with NEBNext Quick Ligation Reaction Buffer (New England Biolabs). The Long Fragment Buffer of the Ligation Sequencing Kit was used during the following wash procedure. The prepared library was sequenced using MinION with the Flow Cell R9.4.1 (Oxford Nanopore Technologies). All samples were technically triplicated.

Reads were base called using Guppy v5.0.11 with dna_r9.4.1_450bps_sup.cfg as a DNA model, and then they were mapped to the genomic sequence of *COL7A1* (RefSeq Accession # NC_000003.12:c48595302-48564073) using minimap2 2.16-r922 (Heng Li, 2017). Using SAMtools 1.9 (H. Li et al., 2009), information from the reads was mapped to the loci of the two mutations (19630th base of the reference for c.5932C>T, 27712th base for c.8029G>A) and was extracted to generate a pileup output. If a read had base qualities higher than 10 at both loci, the

haplotype was determined and counted by analyzing the combination of the read bases at both loci.

Guide RNAs (gRNAs)

The gRNAs were assembled as a duplex from CRISPR RNAs (crRNAs) and trans-activating crRNAs (IDT, Coralville, IA, USA). The crRNA probes were designed using the Benchling software (https://benchling.com/academic). The sequences are provided in **Supplementary Table S1**.

nCATS

Cas9 enrichment and adapter ligation of DNA samples were performed as described previously (Gilpatrick et al., 2020). They followed the protocol for "Cas9 targeted sequencing" (ENR_9084_v109_revP_04Dec2018). Briefly, gDNA was dephosphorylated by Quick Calf Intestinal Phosphatase (New England Biolabs). Typically, 2-5 µg of gDNA was obtained from the epidermis or dermis of a 5-mm skin. At least 1 µg of gDNA was applied to each reaction, as the protocol recommended 1-10 µg. Cleavage and dA-tailing of dephosphorylated DNA samples were performed using Cas9 ribonucleoprotein

complexes, dATP (New England Biolabs), and Taq polymerase (New England Biolabs) at 37 ˚C for 15 min. Cas9 ribonucleoprotein complexes were assembled with annealed all crRNAs/tracrRNA (IDT), CutSmart buffer (New England Biolabs), and S. pyogenes HiFi Cas9 nuclease (IDT). Adapter Mix (AMX) of Ligation Sequencing Kit SQK-LSK109 (Oxford Nanopore Technologies) was ligated to DNA ends using NEBNext Quick T4 Ligase (New England Biolabs) with Ligation buffer LNB of the Ligation Sequencing Kit (Oxford Nanopore Technologies). The samples were cleaned using AMPure XP beads (Beckman Coulter) and used for library preparation. Then they were applied to sequencing using MinION. The alleles were analyzed as described above. For low yield gDNA isolated from skin samples, three reactions per sample were prepared, pooled before the adapter ligation, and sequenced.

Ethics

The institutional review board of the Hokkaido University Graduate School of Medicine approved all human studies described above (ID: 13-043). The study

was carried out according to the Declaration of Helsinki Principles. The participant provided written informed consent.

RESULTS

Immunofluorescence does not fully validate RM in clinically revertant skin of RDEB-intermediate

We selected a patient with RDEB-intermediate (Has et al., 2020) who expressed clinically revertant skin spots. She was compound heterozygous for c.5932C>T (p.Arg1978Ter) and c.8029G>A (p.Gly2677Ser) in *COL7A1* (NM_000094.3) (Natsuga et al., 2010). The former nonsense mutation was expected to lead to NMD, whereas the latter missense mutation did not affect transcripts. Type VII collagen (COL7), encoded by *COL7A1*, was present at the dermoepidermal junction in both her clinically revertant and non-revertant skin, as shown in **Figure 1a.** This was expected according to the mutation profiles. However, the COL7 labeling of non-revertant RDEB skin was slightly weaker than that of normal human skin or clinically revertant RDEB skin (**Figure 1b, Supplementary Figure S1**). This observation was consistent with the previous immunofluorescence studies conducted on this patient's skin (Matsumura et al., 2019; Natsuga et al., 2010), and it illustrates the difficulty of fully confirming RM by immunofluorescence analysis of clinically revertant skin alone.

MinION sequencing differentiates mutant and wild-type alleles

Since RM validation was difficult to perform by immunofluorescence analysis, the next step required the application of genetic methods using nucleic acids for validation. The previously proposed method entailed amplification and sequencing of the target gene's cDNA (Matsumura et al., 2019), but that method could be skewed by artificial recombination between haplotypes during PCR and reverse transcription. Bias could be also formed by NMD in the mRNA derived from one haplotype harboring c.5932C>T (p.Arg1978Ter), as in our case. We reasoned that long-read sequencing at the gDNA level could avoid both issues of artificial recombination and NMD. Therefore, this study employed MinION (Oxford Nanopore Technologies) for this purpose. Sequence reads produced by MinION can be longer than 10 kb, which sufficiently covers both mutational loci of our samples.

We first investigated whether MinION sequencing could quantify the fraction of haplotypes by using artificial mixtures of wild-type (WT) and mutant DNA fragments (**Figure 2a**). The distance between c.5932C>T and c.8029G>A in *COL7A1* is 8082 bp at the gDNA level. We prepared plasmids containing *COL7A1* sequence of WT, c.5932C>T, or c.8029G>A as displayed in **Figure 2a**

and extracted around 8.3 kb DNA fragments from each clone by restriction digestion. The DNA fragments of WT and mutants were combined in various ratios, simulating a mixture of WT and compound heterozygous states. DNA mixtures were used for library construction and sequenced by MinION. Then, each haplotype on a single read that covered both mutational loci was counted. The standard curve of 1% or more WT input was linear (**Figure 2b**), while we observed more than 1% output for WT even when the input WT was lower than 1% (**Figure 2c**). This observation suggests that MinION sequencing can quantify allele frequencies greater than or equal to 1%, but it is difficult to quantify any allele frequency lower than 1%, which is highly likely to be due to the error rate of MinION sequencing.

Long-range PCR technically induces recombination

We then applied MinION sequencing to analyze long-range PCR products (8.3 kb) on gDNA extracted from the revertant and non-revertant epidermis and dermis (**Figure 3a**). The number of PCR cycles (i.e., 35 cycles) was determined to fulfill the DNA amounts necessary for the sequencing procedures. In non-revertant epidermis or dermis and revertant dermis, the reads with c.5932C>T

or c.8029G>A single-mutant alleles were predominant. In contrast, the reads with WT or double-mutant alleles harboring both c.5932C>T and c.8029G>A were higher only in the revertant epidermis (**Figure 3b**), revealing RM in the clinically revertant skin.

Although the results suggested RM, unexpected fractions of WT and double-mutant alleles were detected in non-revertant epidermis and dermis, as displayed in **Figure 3b**. These results imply that artificial recombination between single-mutant haplotypes occurs during PCR procedures (Meyerhans et al., 1990). To test this hypothesis, we prepared long-range PCR products with amplified gDNA extracted from the peripheral blood of the patient, where spontaneous recombination should be minimal. Using different numbers of PCR cycles, we compared the fraction of haplotypes using MinION. At 25 cycles, the reads were almost occupied by c.5932C>T and c.8029G>A single mutants. However, at 30 or 35 cycles, 10 %–30 % WT and double mutant reads emerged (**Figure 4**). The increase in recombination reads from 30 to 35 cycles was not as great as that from 25 to 30 cycles, probably because PCR efficiency was reduced after 30 PCR cycles due to substrate depletion. These results demonstrate that polymerase induces artificial recombination in long-range

PCR, and that recombination is pronounced when the number of PCR cycles is increased.

Cas9-targeted sequencing accurately identifies RM

The data so far point to the need for gDNA sequencing without PCR amplification to identify RM more accurately. We assessed the feasibility of nCATS. It enriches reads from specific genomic regions using Cas9 nuclease and MinION sequencing, and it enables the analysis of long targeted genomic regions without PCR amplification (Gilpatrick et al., 2020) (**Figure 5a**). nCATS successfully enriched the region over 8 kb in *COL7A1* gDNA spanning nucleotide 5932 and 8029 at cDNA level from normal human peripheral blood (**Figure 5b**). We applied this method to the revertant and non-revertant epidermis and dermis of the patient (**Table 1**). nCATS clearly showed that c.5932C>T and c.8029G>A single mutants occupied non-revertant epidermis or dermis and revertant dermis as expected. By contrast, more than 80 % of the reads were WT or double mutant in the revertant epidermis (**Figure 5c, Supplementary Table S2**). Reads with double-mutant alleles indicated intragenic crossover as a primary RM mechanism at this revertant spot (**Figure**

5d). These data point to the superiority of nCATS over the PCR-based method for detecting RM.

DISCUSSION

Previous genetic analyses have identified gene conversion, which is a unidirectional transfer of genetic material from the donor to the acceptor sequences, as one of the RM mechanisms in EB skin (Almaani et al., 2010; Jonkman & Pasmooij, 2009; Jonkman et al., 1997; Kiritsi et al., 2014; Matsumura et al., 2019; Pasmooij et al., 2005). By using nCATS, our study has demonstrated that intragenic crossover, a reciprocal transfer of genetic material between the donor and acceptor sequences, also can lead to RM in EB skin (**Figure 5c-d**). The loss of heterozygosity (LOH) screening using SNP or microsatellite analysis at the gDNA level has been used to detect gene conversion. However, the intragenic crossover cannot be identified by this method because of the absence of LOH. nCATS overcomes this obstacle by analyzing alleles at two separated loci on gDNA simultaneously using targeted long-read sequencing. Without a measure like this, the intragenic crossover, which might be a more common mechanism for RM in EB skin than previously expected, can be overlooked by conventional analysis.

Further advantages of nCATS on gDNA are 1) It can exclude artificial recombination from reverse transcription or PCR amplification at the cDNA or

gDNA level (**Figure 4**); 2) Up to a few tens of kb can be targeted (Gilpatrick et al., 2020); 3) Back mutations, which nullify the inherited pathogenic mutations, and gene conversion can be distinguished as long as some polymorphisms mark heterozygosity in the region of interest; 4) Second-site mutations that ameliorate the pathogenic mutations can be detected if they are present in the enriched region.

One technical issue that might hinder nCATS from validating RM in the skin is that the sequencing needs a few micrograms of gDNA for a reaction, and the laser microdissection technique used in previous studies (Darling et al., 1999; Jonkman & Pasmooij, 2009; Kiritsi et al., 2014; Kiritsi et al., 2012; Kowalewski et al., 2016; Pasmooij et al., 2010; Pasmooij et al., 2012; Pasmooij et al., 2007; Pasmooij et al., 2005; van den Akker et al., 2012) does not generally yield such an amount. Even in our experiments, the epidermis or dermis from a 5-mm skin sample yielded only 2-5 μg of gDNA, which is slightly above the minimum DNA amount required for a single nCATS experiment. In addition, HR detection by nCATS would not be possible in cases with compound heterozygous mutations that are far from each other (> 50 kb) in a

gene. These problems might be solved by further advances in long-read sequencing technologies.

Our result of RM being detected mostly in the epidermis and not in the dermis is consistent with previous studies that identified RM exclusively in the epidermis of recessive dystrophic EB (RDEB) patients (Almaani et al., 2010; Kiritsi et al., 2014; Matsumura et al., 2019; Pasmooij et al., 2010; Tolar et al., 2014; van den Akker et al., 2012). In contrast, only one study has suggested RM in the dermis of an RDEB patient (Twaroski et al., 2019). Our study analyzed more reads from the dermis than from the epidermis (**Table 1**), while the reads with recombination were predominant in the epidermis (**Figure 5c, Supplementary Table S2**), highlighting the epidermis as a major source of RM. The clonal expansion of a genetically reverted cell is required in order to form an intact skin spot in EB. The preference of the epidermis to the dermis in detecting RM might suggest that epidermal keratinocytes have a greater chance to undergo somatic mutations and/or clonal expansion once a cell has genetically reverted.

In summary, our study has shown that nCATS improved RM detection at the gDNA level without being affected by NMD or technically induced

recombination. Clinically revertant skin has been used for cultured epidermal autografts to treat EB (Matsumura et al., 2019). Applying nCATS to cultured epidermis before treatment might benefit EB patients by eliminating the need to transplant autologous epidermis that looks revertant clinically but is not revertant genetically.

Data Availability

All sequence data produced by MinION sequencers and haplotype count data were deposited to Gene Expression Omnibus (GEO) with accession no. GSE186002 (https://www.ncbi.nlm.nih.gov/geo/query/acc.cgi?acc=GSE186002).

CONFLICT OF INTEREST

None to declare.

ACKNOWLEDGEMENTS

We thank Ms. Megumi Takehara for her technical assistance. This work was supported by the World-leading Innovative and Smart Education (WISE) Program (1801) from the Ministry of Education, Culture, Sports, Science, and Technology, Japan.

REFERENCES

Almaani, N., Nagy, N., Liu, L., Dopping-Hepenstal, P. J., Lai-Cheong, J. E., Clements, S. E., . . . McGrath, J. A. (2010). Revertant mosaicism in recessive dystrophic epidermolysis bullosa. *J Invest Dermatol, 130*(7), 1937-1940. doi:10.1038/jid.2010.64

Darling, T. N., Yee, C., Bauer, J. W., Hintner, H., & Yancey, K. B. (1999). Revertant mosaicism: partial correction of a germ-line mutation in COL17A1 by a frame-restoring mutation. *J Clin Invest, 103*(10), 1371-1377. doi:10.1172/JCI4338

Gilpatrick, T., Lee, I., Graham, J. E., Raimondeau, E., Bowen, R., Heron, A., . . . Timp, W. (2020). Targeted nanopore sequencing with Cas9-guided adapter ligation. *Nat Biotechnol, 38*(4), 433-438. doi:10.1038/s41587-020-0407-5

Has, C., Bauer, J. W., Bodemer, C., Bolling, M. C., Bruckner-Tuderman, L., Diem, A., . . . Mellerio, J. E. (2020). Consensus reclassification of inherited epidermolysis bullosa and other disorders with skin fragility. *Br J Dermatol, 183*(4), 614-627. doi:10.1111/bjd.18921

Jonkman, M. F., & Pasmooij, A. M. (2009). Revertant mosaicism--patchwork in the skin. *N Engl J Med, 360*(16), 1680-1682. doi:10.1056/NEJMc0809896

Jonkman, M. F., Scheffer, H., Stulp, R., Pas, H. H., Nijenhuis, M., Heeres, K., . . . Uitto, J. (1997). Revertant mosaicism in epidermolysis bullosa caused by mitotic gene conversion. *Cell, 88*(4), 543-551. doi:10.1016/s0092-8674(00)81894-2

Kiritsi, D., Garcia, M., Brander, R., Has, C., Meijer, R., Jose Escamez, M., . . . Pasmooij, A. M. G. (2014). Mechanisms of natural gene therapy in dystrophic epidermolysis bullosa. *J Invest Dermatol, 134*(8), 2097-2104. doi:10.1038/jid.2014.118

Kiritsi, D., He, Y., Pasmooij, A. M., Onder, M., Happle, R., Jonkman, M. F., . . . Has, C. (2012). Revertant mosaicism in a human skin fragility disorder results from slipped mispairing and mitotic recombination. *J Clin Invest, 122*(5), 1742-1746. doi:10.1172/JCI61976

Kowalewski, C., Bremer, J., Gostynski, A., Wertheim-Tysarowska, K., Wozniak, K., Bal, J., . . . Pasmooij, A. M. (2016). Amelioration of junctional

epidermolysis bullosa due to exon skipping. *Br J Dermatol, 174*(6), 1375-1379. doi:10.1111/bjd.14374

Lai-Cheong, J. E., Moss, C., Parsons, M., Almaani, N., & McGrath, J. A. (2012). Revertant mosaicism in Kindler syndrome. *J Invest Dermatol, 132*(3 Pt 1), 730-732. doi:10.1038/jid.2011.352

Li, H. (2017). Minimap2: pairwise alignment for nucleotide sequences. arXiv:1708.01492. Retrieved from https://ui.adsabs.harvard.edu/abs/2017arXiv170801492L

Li, H., Handsaker, B., Wysoker, A., Fennell, T., Ruan, J., Homer, N., . . . Genome Project Data Processing, S. (2009). The Sequence Alignment/Map format and SAMtools. *Bioinformatics, 25*(16), 2078-2079. doi:10.1093/bioinformatics/btp352

Matsumura, W., Fujita, Y., Shinkuma, S., Suzuki, S., Yokoshiki, S., Goto, H., . . . Shimizu, H. (2019). Cultured Epidermal Autografts from Clinically Revertant Skin as a Potential Wound Treatment for Recessive Dystrophic Epidermolysis Bullosa. *J Invest Dermatol, 139*(10), 2115-2124. doi:10.1016/j.jid.2019.03.1155

Meyerhans, A., Vartanian, J. P., & Wain-Hobson, S. (1990). DNA recombination during PCR. *Nucleic Acids Res, 18*(7), 1687-1691. doi:10.1093/nar/18.7.1687

Natsuga, K., Sawamura, D., Goto, M., Homma, E., Goto-Ohguchi, Y., Aoyagi, S., . . . Shimizu, H. (2010). Response of intractable skin ulcers in recessive dystrophic epidermolysis bullosa patients to an allogeneic cultured dermal substitute. *Acta Derm Venereol, 90*(2), 165-169. doi:10.2340/00015555-0776

Negroni, M., Ricchetti, M., Nouvel, P., & Buc, H. (1995). Homologous recombination promoted by reverse transcriptase during copying of two distinct RNA templates. *Proc Natl Acad Sci U S A, 92*(15), 6971-6975. doi:10.1073/pnas.92.15.6971

Nomura, T. (2020). Recombination-induced revertant mosaicism in ichthyosis with confetti and loricrin keratoderma. *J Dermatol Sci, 97*(2), 94-100. doi:10.1016/j.jdermsci.2019.12.013

Pasmooij, A. M., Garcia, M., Escamez, M. J., Nijenhuis, A. M., Azon, A., Cuadrado-Corrales, N., . . . Del Rio, M. (2010). Revertant mosaicism due to a second-site mutation in COL7A1 in a patient with recessive

dystrophic epidermolysis bullosa. *J Invest Dermatol, 130*(10), 2407-2411. doi:10.1038/jid.2010.163

Pasmooij, A. M., Nijenhuis, M., Brander, R., & Jonkman, M. F. (2012). Natural gene therapy may occur in all patients with generalized non-Herlitz junctional epidermolysis bullosa with COL17A1 mutations. *J Invest Dermatol, 132*(5), 1374-1383. doi:10.1038/jid.2011.477

Pasmooij, A. M., Pas, H. H., Bolling, M. C., & Jonkman, M. F. (2007). Revertant mosaicism in junctional epidermolysis bullosa due to multiple correcting second-site mutations in LAMB3. *J Clin Invest, 117*(5), 1240-1248. doi:10.1172/JCI30465

Pasmooij, A. M., Pas, H. H., Deviaene, F. C., Nijenhuis, M., & Jonkman, M. F. (2005). Multiple correcting COL17A1 mutations in patients with revertant mosaicism of epidermolysis bullosa. *Am J Hum Genet, 77*(5), 727-740. doi:10.1086/497344

Schuilenga-Hut, P. H., Scheffer, H., Pas, H. H., Nijenhuis, M., Buys, C. H., & Jonkman, M. F. (2002). Partial revertant mosaicism of keratin 14 in a patient with recessive epidermolysis bullosa simplex. *J Invest Dermatol, 118*(4), 626-630. doi:10.1046/j.1523-1747.2002.01715.x

Smith, F. J., Morley, S. M., & McLean, W. H. (2004). Novel mechanism of revertant mosaicism in Dowling-Meara epidermolysis bullosa simplex. *J Invest Dermatol, 122*(1), 73-77. doi:10.1046/j.0022-202X.2003.22129.x

Stangl, C., de Blank, S., Renkens, I., Westera, L., Verbeek, T., Valle-Inclan, J. E., . . . Monroe, G. R. (2020). Partner independent fusion gene detection by multiplexed CRISPR-Cas9 enrichment and long read nanopore sequencing. *Nature Communications, 11*(1), 2861. doi:10.1038/s41467-020-16641-7

Tolar, J., McGrath, J. A., Xia, L., Riddle, M. J., Lees, C. J., Eide, C., . . . Wagner, J. E. (2014). Patient-specific naturally gene-reverted induced pluripotent stem cells in recessive dystrophic epidermolysis bullosa. *J Invest Dermatol, 134*(5), 1246-1254. doi:10.1038/jid.2013.523

Twaroski, K., Eide, C., Riddle, M. J., Xia, L., Lees, C. J., Chen, W., . . . Tolar, J. (2019). Revertant mosaic fibroblasts in recessive dystrophic epidermolysis bullosa. *Br J Dermatol, 181*(6), 1247-1253. doi:10.1111/bjd.17943

van den Akker, P. C., Nijenhuis, M., Meijer, G., Hofstra, R. M., Jonkman, M. F., & Pasmooij, A. M. (2012). Natural gene therapy in dystrophic

epidermolysis bullosa. *Arch Dermatol, 148*(2), 213-216. doi:10.1001/archdermatol.2011.298

Watson, C. M., Crinnion, L. A., Hewitt, S., Bates, J., Robinson, R., Carr, I. M., . . . Bonthron, D. T. (2020). Cas9-based enrichment and single-molecule sequencing for precise characterization of genomic duplications. *Laboratory Investigation, 100*(1), 135-146. doi:10.1038/s41374-019-0283-0

Wongsurawat, T., Jenjaroenpun, P., De Loose, A., Alkam, D., Ussery, D. W., Nookaew, I., . . . Rodriguez, A. (2020). A novel Cas9-targeted long-read assay for simultaneous detection of IDH1/2 mutations and clinically relevant MGMT methylation in fresh biopsies of diffuse glioma. *Acta Neuropathologica Communications, 8*(1), 87. doi:10.1186/s40478-020-00963-0

FIGURE LEGENDS

Figure 1. Clinically revertant skin in an RDEB patient.

(a) An RDEB patient with compound heterozygous mutations in *COL7A1*. Clinically revertant skin on her upper arm is encircled by the dotted line. (b) COL7 labeling of clinically revertant and non-revertant skin samples (primary antibody LH7.2 dilution: 1/400). Bar = 100 μm.

Figure 2. Accuracy of MinION sequencing.

(a) Mixtures of plasmids containing *COL7A1* gDNA sequences covering nucleotides 5932 and 8029 at the cDNA level. (b) A linear-scale calibration curve for input and output WT%. (c) A log-scale calibration curve for input and output WT%.

Figure 3. RM detection on long-range PCR products by MinION sequencing.

(a) Diagram of the PCR strategy. (b) Frequency of WT (CG), single-mutant (TG or CA, corresponding to c.5932C>T or c.8029G>A, respectively), and double-mutant (TA, harboring c.5932C>T and c.8029G>A in one allele) reads. PCR products from clinically revertant and non-revertant epidermis/dermis gDNA are analyzed.

Figure 4. Recombination technically induced by PCR.

Frequency of WT (CG), single-mutant (TG or CA, corresponding to c.5932C>T or c.8029G>A, respectively), and double-mutant (TA, harboring c.5932C>T and c.8029G>A in one allele) reads. PCR products from normal human epidermis and the patient's peripheral blood (PB) gDNA were analyzed by MinION sequencing. PCR cycles of 25, 30, and 35 are shown.

Figure 5. RM detection by nanopore Cas9-targeted sequencing (nCATS).

(a) Diagram of nCATS. Six gRNAs are designed to target the gene region harboring the two *COL7A1*, following the procedure of the previous report (Gilpatrick et al., 2020). (b) Coverage plots at the *COL7A1* gene (enriched area 9 kb). (c) Frequency of WT (CG), single-mutant (TG or CA, corresponding to c.5932C>T or c.8029G>A, respectively), and double-mutant (TA, harboring c.5932C>T and c.8029G>A in one allele) reads. Cas9-targeted gDNA from normal human epidermis, clinically revertant dermis and epidermis, and non-revertant dermis and epidermis are analyzed. (d) Intragenic crossover as a mechanism of RM in the epidermis.

Table 1. Coverage table of nCATS.

Read counts and on-target percentage are shown.

Figure 1. Clinically revertant skin in an RDEB patient.

a

b

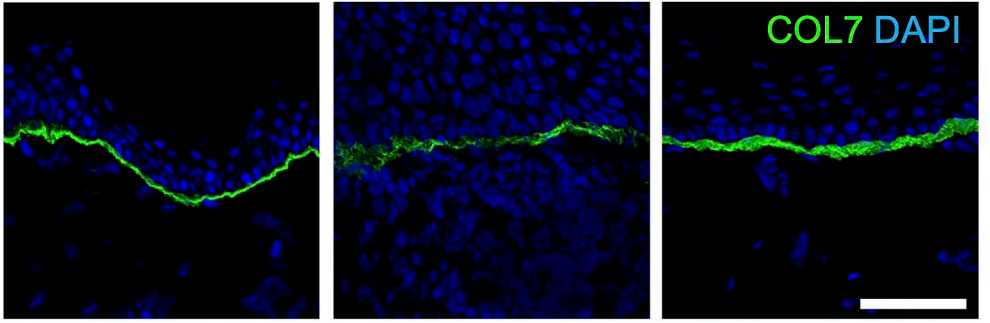

Normal human skin

Non-revertant RDEB skin

Clinically-revertant RDEB skin

Figure 2. Accuracy of MinION sequencing.

a

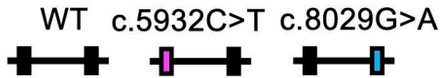

Input WT 0%	0%	50%	50%
Input WT 0.1%	0.1%	49.95%	49.95%
Input WT 1%	1%	49.5%	49.5%
Input WT 10%	10%	45%	45%
Input WT 25%	25%	37.5%	37.5%
Input WT 50%	50%	25%	25%
Input WT 75%	75%	12.5%	12.5%
Input WT 100%	100%	0%	0%

b

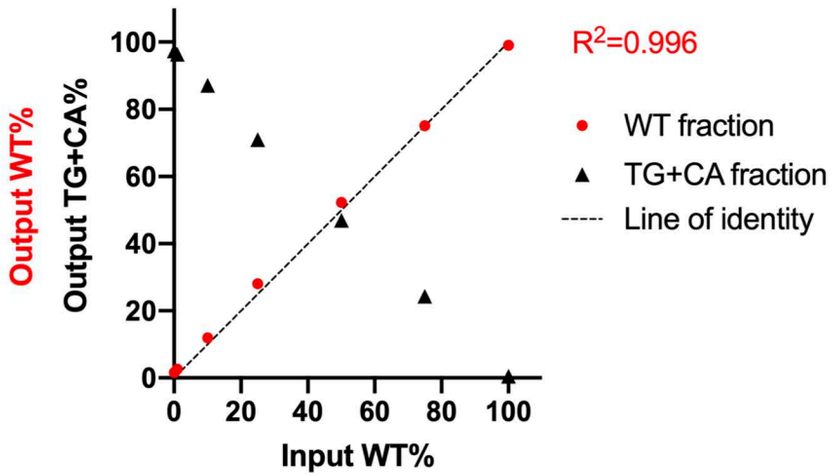

c

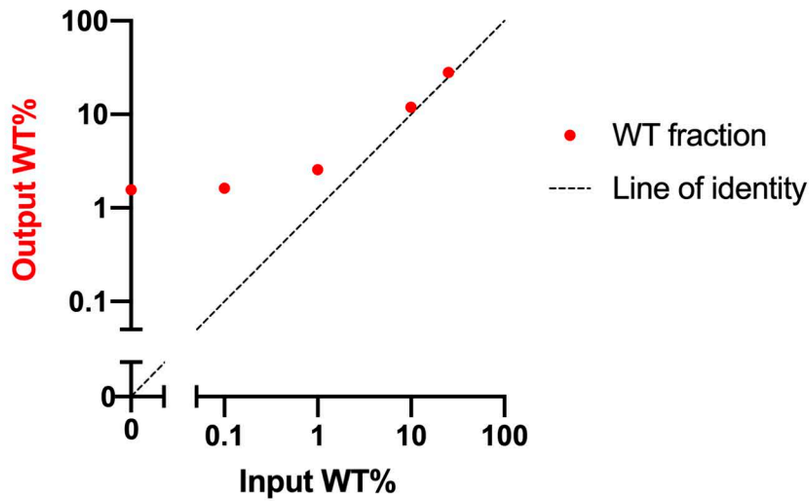

Figure 3. RM detection on long-range PCR products by MinION sequencing

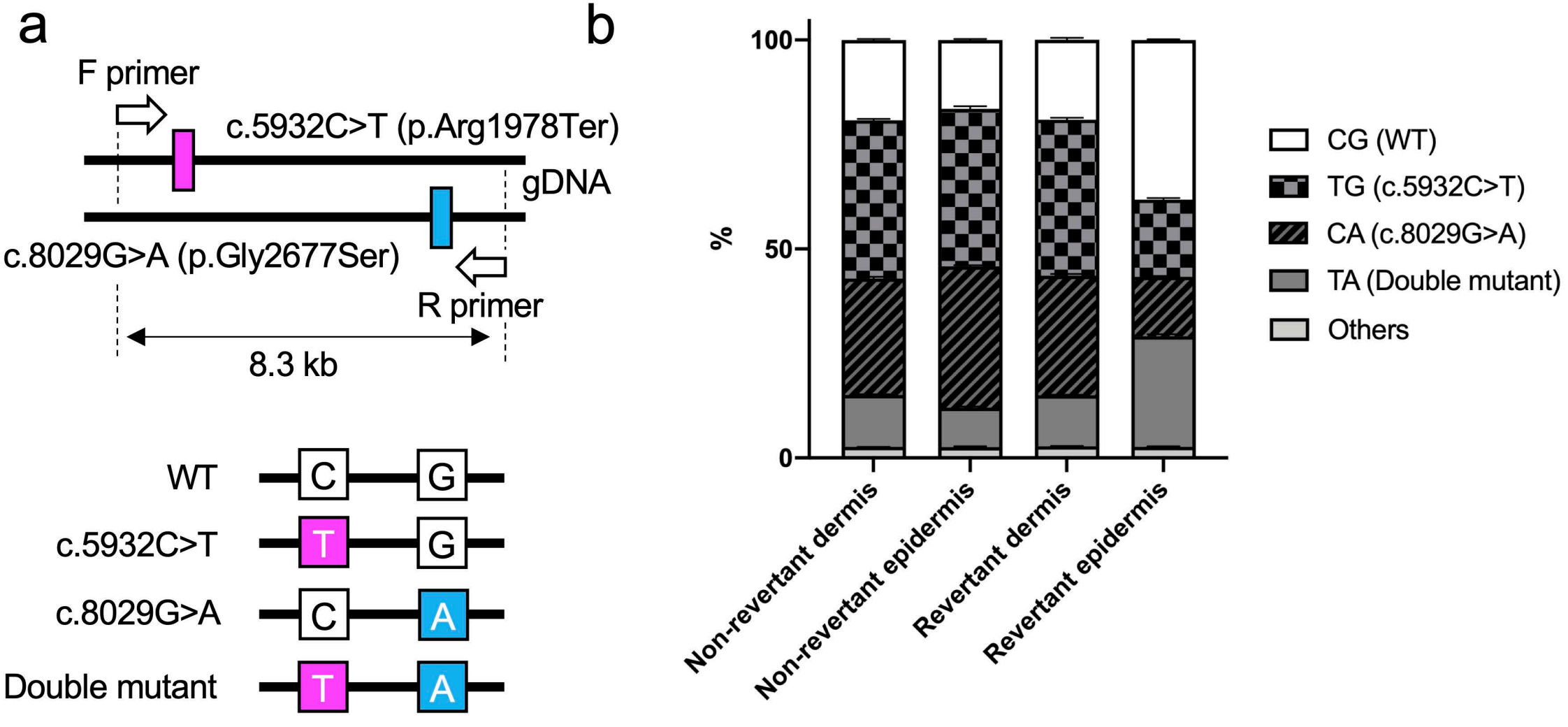

Figure 4. Recombination technically induced by PCR.

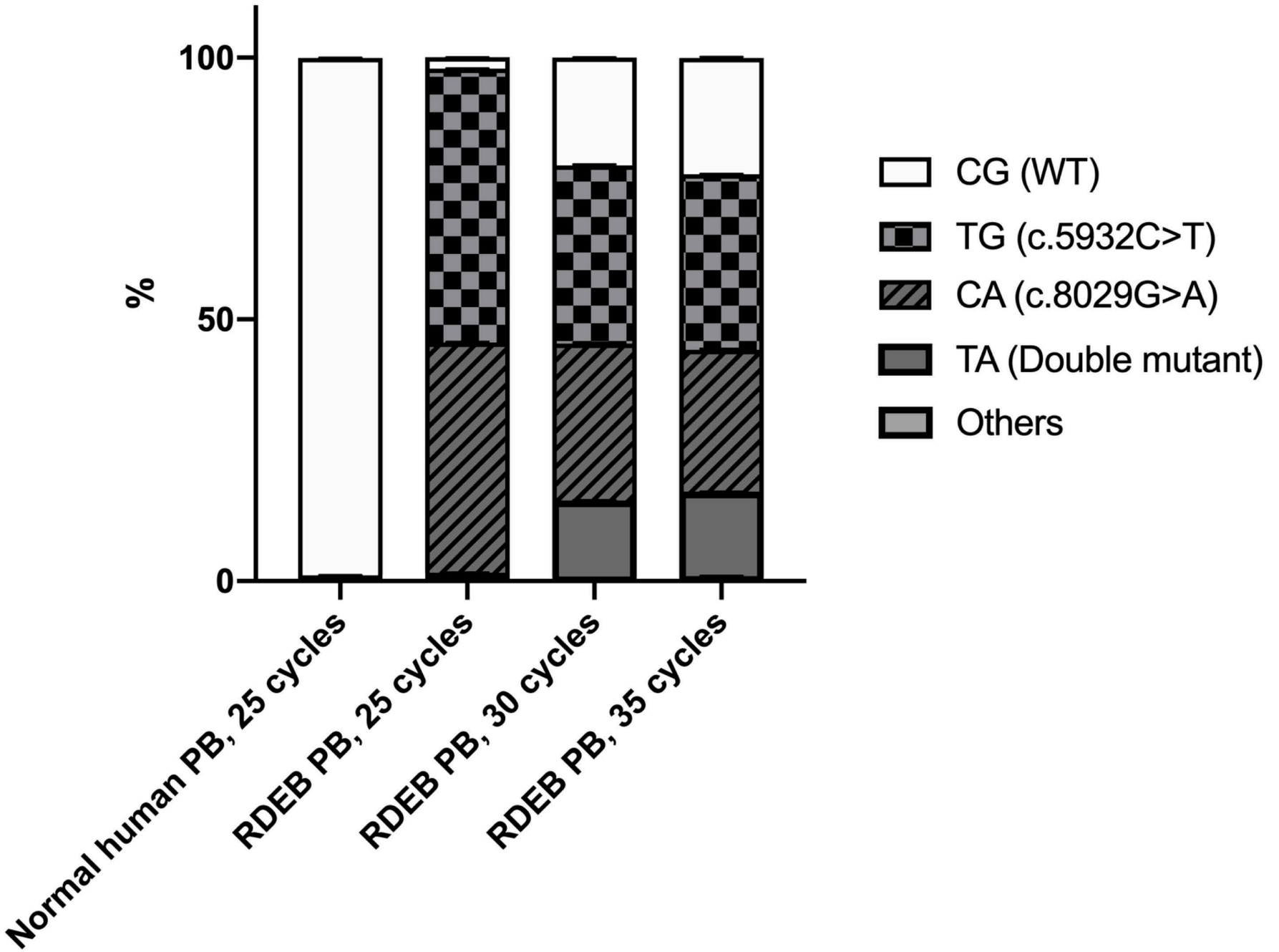

Figure 5. RM detection by nanopore Cas9-targeted sequencing (nCATS).

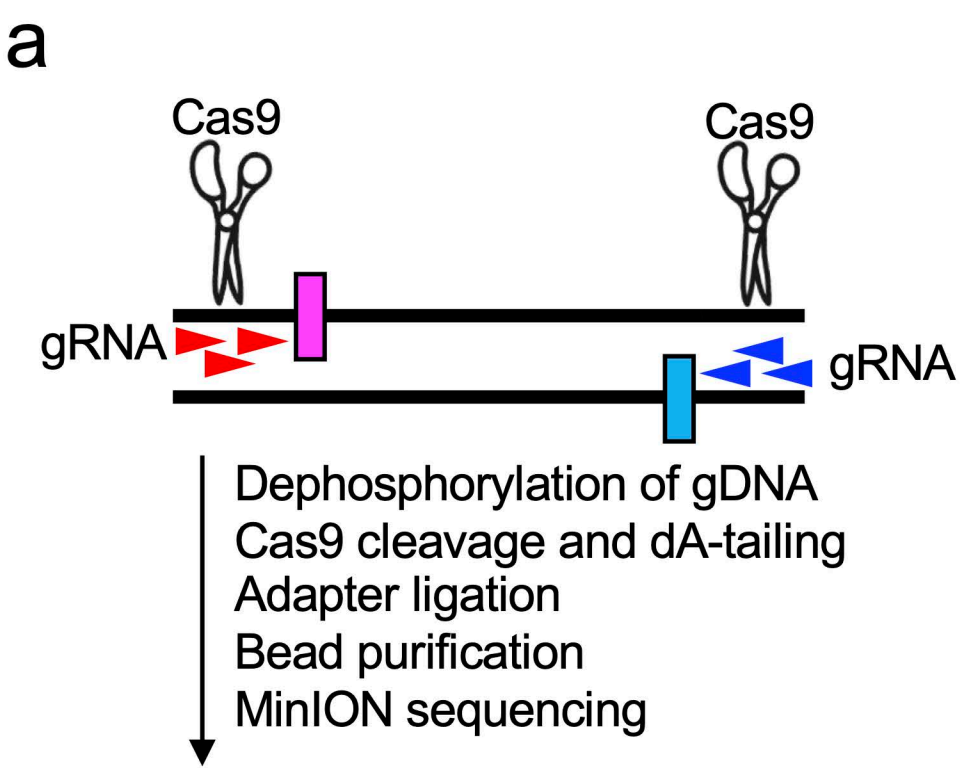

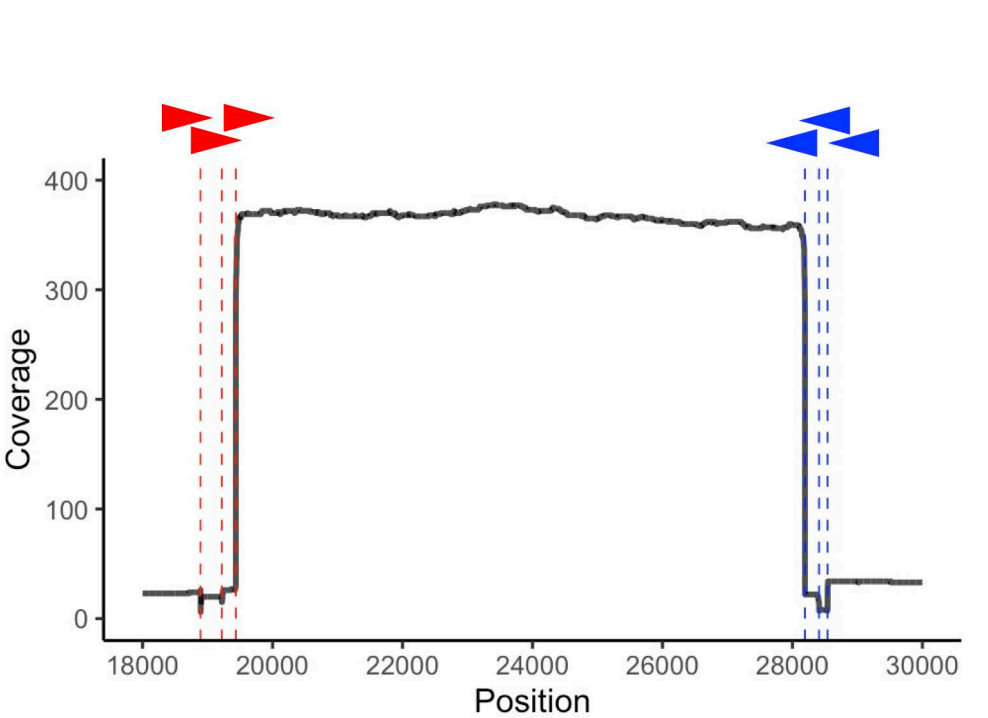

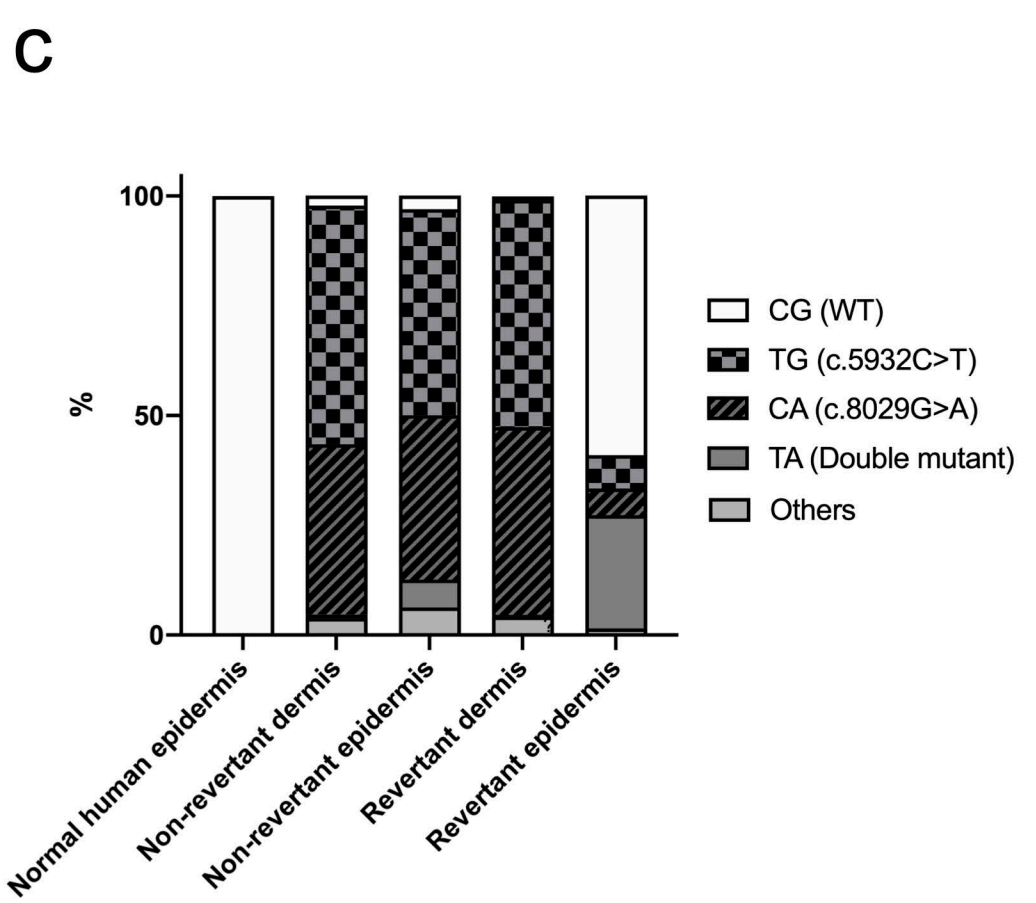

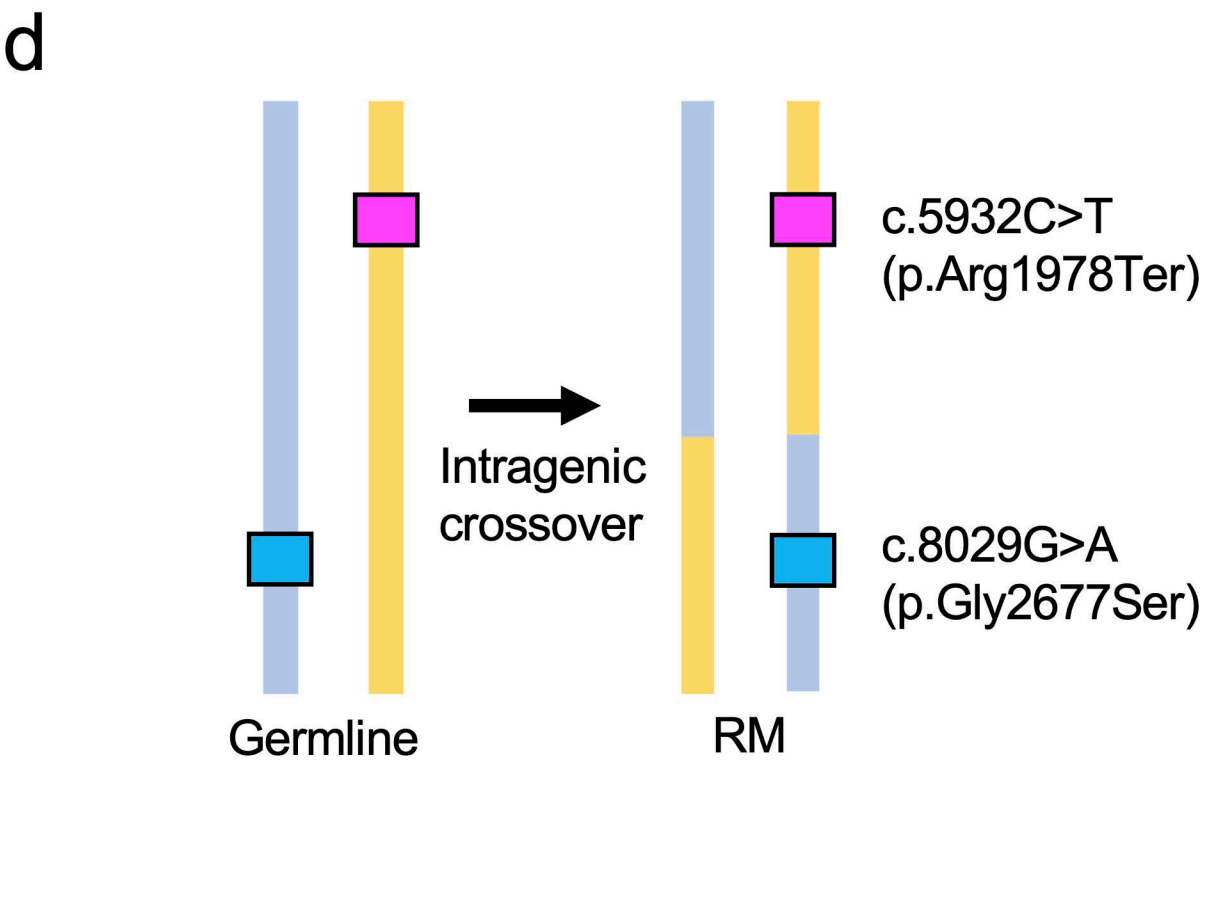

Table 1. Coverage table of nCATS.

Read counts and on-target percentage are shown.

Sample	Read#	Read# mapped in the target region	Read# covered both loci	Read# covered both loci with quality value >10
Normal human epidermis	49161	158 (0.32%)	72 (0.15%)	34 (0.069%)
Non-revertant dermis	174442	797 (0.46%)	284 (0.16%)	129 (0.074%)
Non-revertant epidermis	9163	86 (0.94%)	75 (0.81%)	32 (0.35%)
Revertant dermis	164220	848 (0.52%)	554 (0.33%)	236 (0.14%)
Revertant epidermis	24859	242 (0.97%)	162 (0.65%)	66 (0.27%)